ELSEVIER

S0032-3861(96)00385-0

Polymer Vol. 37 No. 24, pp. 5483–5491, 1996

0032-3861/96/$15.00+0.00

Surface energetics of films of poly(vinyl acetate–butyl acrylate) emulsion copolymers

H. Yıldırım Erbil
TUBITAK, Marmara Research Center, Department of Chemistry, Research Institute for Basic Sciences, PO Box 21, 41470 Gebze-Kocaeli, Turkey
(Received 22 March 1995; revised 17 January 1996)

Vinyl acetate (VA) and butyl acrylate (BA) monomers were emulsion copolymerized by using controlled monomer and initiator addition method. Particle size distributions, viscosity average molecular weights ($\bar{M}_V$), glass-transition temperatures (T_g°) and molar composition of the copolymers were determined. Surface tension components of the copolymer films were calculated from contact angle data of various liquids by using Van Oss–Good methodology. A decrease of average particle size and T_g° was found by the increase of BA content. $\bar{M}_V$ increased up to 40 mol% BA, then decreased. Apolar Lifshitz–Van der Waals surface tension component was not affected by the change in BA content; however, electron donor surface tension coefficient (γ_s^-) decreased considerably with the BA increase. The work of adhesion was calculated for cellulosic substrate–latex film interfaces. Copyright © 1996 Elsevier Science Ltd.

(Keywords: surface free energy; contact angle; emulsion copolymerization)

INTRODUCTION

El-Aasser, Vanderhoff and co-workers have investigated systematically the different effects of batch and semi-continuous copolymerization of vinyl acetate (VA) and butyl acrylate (BA) on latex particle size, molecular weight, latex stability, surface characteristics and the morphological, mechanical properties of their films[1–5]. Since, the water solubilities are quite different (290 and 11 mM for VA and BA respectively[1]), as are the copolymerization reactivity ratios ($r_1 = 0.015$–0.040 for VA and $r_2 = 3.3$–10.7 for BA[6–8]), it is expected that in a typical batch polymerization a polybutylacrylate-rich copolymer is formed until the BA monomer is exhausted and polyvinylacetate is formed thereafter, resulting in a blend of homopolymer latex films when dried. In order to avoid this it was shown that homogeneous copolymer compositions were obtained by a semi-continuous polymerization process where the monomer was added at a rate less than the rate of polymerization[2,8]. Then the copolymer composition per particle was found to represent the composition of the two monomers in the monomer mixture[1–5]. In the semi-continuous process the nucleation stage is long and the greater number of initial particles formed results in smaller particle size and broader particle size distribution. The average particle size of the semi-continuous latexes decreased with increasing BA content[1–4]. Semi-continuous latexes have a broader molecular weight distribution and bimodal distributions were obtained, indicating severe branching. The number-average molecular weights ($\bar{M}_n$) of the semi-continuous latexes were four to ten times smaller than those of batch copolymers. The BA content did not affect $\bar{M}_n$ considerably[1–4]. Only one glass transition temperature (T_g°) was found for the semi-continuous copolymer latex film and the T_g° decreased with the increase of BA content, as expected[4]. Tensile properties of the semi-continuous copolymer films showed a lower ultimate tensile strength, lower Young's modulus and higher percentage elongation to break compared to batch copolymer films[2]. The filming ability was better in semi-continuous copolymer latex films and was enhanced with increased BA content[3]. The addition of BA causes further coalescence of the copolymer latex films, a process known as interdiffusion of polymer molecules across the area of contact of the particles. In the above work, thermal initiation at 75°C was used which was far above the value for commercial semi-continuous polymerizations (~50°C) in which the redox initiators were used to increase molecular weight and to decrease branching.

In addition, the surface free energy (or surface tension) analysis of polymer films is very important from a practical point of view in order to understand their adhesion, coalescence, wettability, and water repellency properties during application. In general, the surface structure of polymers is investigated by X-ray photoelectron spectroscopy (X.p.s.), attenuated total reflectance Fourier transform infra-red spectroscopy (a.t.r. *FT*i.r.) and more practically by the contact angle measurement. The indirect determination of the surface free energy of the polymers by the one-liquid contact angle method (the air–liquid–polymer system) had been proposed by Fowkes[9], Girifalco and Good[10] and Owens and Wendt[11]. The change of the surface free energy properties of the copolymer films with the copolymer composition were determined by applying these semi-empirical approaches[12–14]; later, non-linear programming methods were adopted[15,16].

Recently, Van Oss, Good and co-workers introduced a theory and a practical methodology to estimate the interfacial tension between apolar and electron acceptor, electron donor molecules[17,18]. They assumed that surface and interfacial free energies consisted of two components: an apolar or a Lifshitz–Van der Waals component (indicated by superscript LW) of electrodynamic origin, and a polar component (indicated by superscript AB) caused by acid–base interactions. This methodology was successfully applied to polymers and protein interactions with liquids, surface free energy determinations of polymers, polymer solubility predictions of solvents and critical micelle concentrations of surfactants[17–21]. This approach was also tested with liquid–liquid interactions[22] and the calculated results agreed well with independent interfacial tension data from mercury interactions with the liquids[23].

It is the purpose of this research to study the surface energetics of the poly(vinyl acetate–butyl acrylate) semicontinuous emulsion copolymer system which was produced by using non-ionic emulsifiers, and initiators that allow low temperature initiation. Controlled addition of both the comonomer mixture and the initiators throughout the copolymerization reaction was applied. Another aim is the calculation of the work of adhesion between the produced copolymer film and the cellulosic substrate to determine its variation with the change in the copolymer composition.

EXPERIMENTAL

Materials

Both monomers VA and BA were distilled under vacuum to remove the inhibitor and kept at −10°C in a cooler in brown bottles. Ammonium persulfate and formic acid were reagent grade (Merck) and sodium formaldehyde sulfoxylate was technical grade (Rongalit C of BASF Co.). Nonyl phenol ethoxylate emulsifiers were also technical grade (NP-10 and NP-30 of Türk-Henkel Co.) and were used as received. Deionized water was used in all polymerizations.

Preparation of copolymer latexes

All the emulsion polymerizations were carried out in a 1 litre jacketed split resin flask glass reactor, equipped with a reflux condenser, a mechanical stirrer with two-bladed Teflon propeller and three dropping funnels, one for comonomer mixture and the other two for the two initiator solutions. There were two more inlets on the reactor, one for the dried nitrogen gas and the other for the thermometer probe. The stirring rate was maintained at 150 rev min^{-1} throughout the reactions. The jacket of the reactor was connected with a water circulator which was capable of both cooling and heating. By the help of this set-up the precise adjustment of the temperature of the reaction medium during heating and cooling cycles was carried out. The polymer latexes were prepared using recipes given in *Table 1*. The weight and the molar percentage composition of the comonomer feed are given in *Table 2* according to BA content.

Deionized water and the NP-30 emulsifier were initially charged into the reactor and nitrogen gas was bubbled for 20 min with stirring, then the nitrogen atmosphere was maintained by passing the gas above the solution throughout the reaction. The pH of the solution was adjusted to 4.3 using formic acid solution at 35°C, then 5% of the total monomer mixture was added in 10 min to the solution, the temperature was raised to 40°C, then 10% of the total ammonium persulfate and sodium formaldehyde sulfoxylate initiators (dissolved in deionized water) were added, and the temperature was raised to 50°C within 15 min. The remaining comonomer mixture containing NP-10 emulsifier and the initiator solutions were simultaneously added through the dropping funnels within 4 h. The temperature was held constant at 50°C by cooling the exothermic reaction mixture. After 4 h at a constant rate of addition of monomers and initiators, the reaction mixture was heated to 60°C and held at this temperature for 15 min to consume free monomer and to reach 100% conversion. After cooling, the acidity of the latex was adjusted to pH 6.5 by the addition of NH_3 solution. The final conversion was measured gravimetrically and was found to vary between 96 and 99%. The solids content of the latexes was determined gravimetrically by evaporating the water in preweighed aluminium dishes in an oven at 110°C for 2 h. A mean solids content value of 46.8% was found.

Table 1 Polymerization recipe

	wt%
Monomer mixture	45.00
Deionized water	52.72
NP-10 emulsifier	0.90
NP-30 emulsifier	0.90
Ammonium persulfate	0.28
Sodium formaldehyde sulfoxylate	0.18
Formic acid (1%)	0.02
	100.00

Table 2 Butyl acrylate content in latex samples

Sample	Feed monomer content (wt%)	Feed monomer content (mol%)	Polymer content (mol%)
P1	0	0	0
P2	35.3	26.8	28.2
P3	43.2	33.8	34.7
P4	49.8	40.0	40.3
P5	56.4	46.5	46.9
P6	64.9	55.4	55.8
P7	100.0	100.0	100.0

Viscosity-average molecular weight

All the dried copolymer samples were dissolved in ultra-pure acetone solvent. An Ubbelohde type capillary viscometer (Shott-Gerate No. 50) was used to determine the intrinsic viscosity of the samples at 25°C. $\bar{M}_V$ values were calculated by the application of the Mark–Houwink equation:

$$[\eta] = K\bar{M}_V^a \quad (1)$$

using values of $K = 6.85 \times 10^{-5}$ and $a = 0.75$ for BA homopolymer[24]. Since we could not find the Mark–Houwink constants for VA–BA copolymers in the existing literature and the constants for poly(vinyl acetate) homopolymer ($K = 10.8 \times 10^{-5}$ and $a = 0.72$)[24] are close to the constants of poly(butyl acrylate) homopolymer, we preferred to use the above data as a rough guide to the copolymer molecular weight.

Nuclear magnetic resonance spectra

The composition of the copolymer films was obtained from nuclear magnetic resonance (n.m.r.) spectra using Bruker AC200L spectrometer (200 MHz for ^1H) and recorded at 21°C. Saturated deuterated benzene solution was used. The copolymer compositions were calculated from the relative intensities by direct integration of the CH group resonance in vinyl acetate at 5.22 ppm and $-O-CH_2$ group resonance in butyl acrylate at 4.13 ppm. The equation given by Bataille and Bourassa[6] was used.

Particle size measurement

Particle size distributions and the average particle sizes were measured by laser scattering using Malvern-3 Zetasizer instrument. The measurements were carried out at 25°C in double-distilled water.

Glass transition temperature measurement

The glass transition temperatures of the copolymer samples were measured by using a DuPont DSC Analyzer 910 instrument at a heating rate of 10°C min^{-1} (sample P7, having 100% BA content, could not be measured owing to its very low temperature value so it was taken from literature[4]).

Latex viscosity

The latex solid contents were adjusted to 42% by adding enough water, then their viscosities were measured by using Brookfield LV instrument with Spindle no. 1, at 60 rev min^{-1} at 20°C.

Contact angle measurements

The one-liquid method (air–liquid drop–polymer system) was used. The contact angles of water, glycerol, ethylene glycol, formamide, paraffin oil and decalin drops were measured by using a Kernco Model G-III contact angle meter at 25°C. Only advancing angles were determined. The average of three measurements was reported and it deviated within ±2°.

RESULTS

Copolymer structure

Poly(butyl acrylate) content in poly(vinyl acetate–butyl acrylate) copolymer samples determined from n.m.r. measurements is presented in *Table 2*. As seen from this table, poly(BA) content deviated from 0.7 to 5.2% from the feed BA monomer mole content. This result confirms the general belief that the bulk copolymer structure is very similar to the feed monomer composition in semi-continuous copolymerizations.

Viscosity-average molecular weight of copolymers

Experimental $\bar{M}_V$ results are presented in *Table 3* and *Figure 1*. The use of ammonium persulfate–sodium formaldehyde sulfoxylate system produces sulfite anion-radicals instead of sulfate anion-radicals of thermal bond scission of persulfate as shown below:

$$S_2O_8^{2-} + HOCH_2SO_2^- + OH^- \rightarrow 2(HCHO)SO_3^- \cdot + H_2O$$

$$S_2O_8^{-2} \xrightarrow[\Delta]{} 2SO_4^- \cdot$$

Advantages of using lower polymerization temperatures include better control of polymerization rates,

Table 3 Viscosity-average molecular weight, mean particle size, glass transition temperature and Brookfield viscosity of the copolymer samples

Sample	BuAc (mol%)	$\bar{M}_V$ ($\times 10^3$)	$\bar{D}_p$ (Å)	T_g (°C)	η (cP)
P1	0	204	4750	29	630
P2	26.8	265	2150	6	12
P3	33.8	432	2530	0	160
P4	40.0	612	1600	−9	14
P5	46.5	560	1580	−13	15
P6	55.4	530	1370	−27	30
P7	100.0	480	860	−63	14

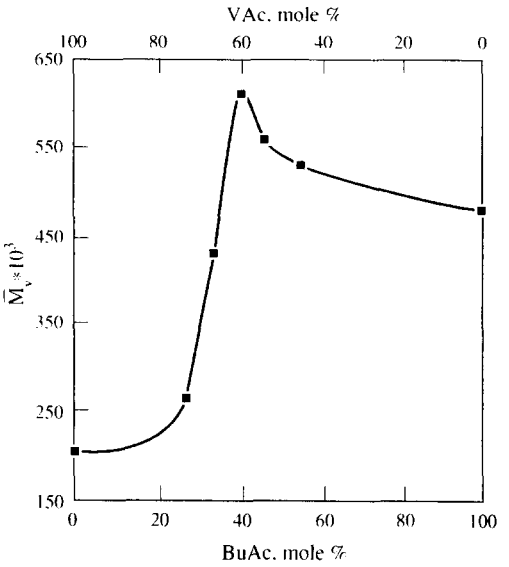

Figure 1 Change of viscosity average molecular weights with the BA content of VA–BA copolymers

suppression of side reactions (grafting due to transfer to polymer), and higher resulting polymer molecular weight. The advantage of a redox initiation system lies in the much lower activation energy for bond scission, about 10 kcal mol^{-1} compared to 30–35 kcal mol^{-1} required in thermal scission.

As VA monomer is highly water soluble, it is generally accepted that the initiation begins in the aqueous phase[1,8]. In this system, radicals generated in the aqueous phase add monomer units until the oligomeric radicals exceed their solubility and precipitate. The precipitated oligomeric radicals form spherical particles which adsorb emulsifier and monomer to become primary particles. These primary particles flocculate with already existing particles. In this system the function of the emulsifier is to stabilize the particles precipitating from the aqueous phase[1,7,8]. The polymerization of sample P1 is assumed to begin with this mechanism.

On the other hand, monomers which are less soluble in water such as BA polymerize with the initiation in monomer-swollen micelles system. In this system the radicals generated in the aqueous phase enter monomer-swollen micelles and initiate polymerization to form a monomer-swollen polymer particle. Only one of every 100–1000 micelles captures a radical and becomes a polymer particle; the others give up their monomer and emulsifier to neighbouring micelles which have captured

a radical. The monomer droplets act as reservoirs feeding monomer to the micelles and polymer particles by diffusion through the aqueous phase[1,8]. It is assumed that sample P7 was polymerized by this mechanism. The other samples, P2 to P6, should polymerize with a system which is intermediate between both systems.

The $\bar{M}_V$ values for the copolymer samples were dependent upon the BA content as seen in *Figure 1*. It increased with the increase of BA content up to 40 mol%, after showing a peak at 40 mol%, then it decreased slowly exhibiting a plateau between 60 and 100% BA content. The trend is somewhat similar to $\bar{M}_n$ (number-average molecular weight) results of El-Aasser, Vanderhoff and co-workers[1,3,4] which exhibit two peaks at 11 and 51% BA for overall semi-continuous samples by using g.p.c. They attributed the broad and bimodal $\bar{M}_n$ distribution of the copolymers to the presence of the low-molecular weight (MW) oligomers and high-MW long-chain branches. They assumed that the presence of low-MW oligomers may be due to the lower monomer concentration at the site of polymerization and predominant initiation in the aqueous phase[1,25]. Since we determined only the viscosity-average MW of the copolymers, which does not give direct information on branching, we can only indicate that the copolymers having 34 to 100 mol% BA content have a $\bar{M}_V$ value which was nearly two to three times that of the poly(vinyl acetate) homopolymer.

Particle size of copolymers

The Zetasizer instrument calculates and reports the *Z*-average particle size and polydispersity using the cumulants method. The instrument determines the velocities of all the particles in the latex as they undergo Brownian diffusion, and calculates the particle diameter from the diffusion coefficient using the Stokes–Einstein equation. The mean particle sizes ($\bar{D}_p$) are reported in *Table 3*. The change of $\bar{D}_p$ with the increase of BA content of copolymers is given in *Figure 2*. The mean diameter was found to decrease with increasing BA content. When BA content is high in comonomer mixtures, the more hydrophobic BA monomer favours the adsorption of emulsifier on the particle surface which results in a higher number of newly formed small latex particles having a high level of colloidal stability. Thus, copolymers having high BA contents were composed of particles with small average size. On the other hand, when hydrophilic VA content increase, this inhibits the adsorption of emulsifier on the particle surface resulting in less stable particles which tend to coalesce, thus giving large size particles. The trend of $\bar{D}_p$ decrease with BA increase is similar to the results of El-Aasser, Vanderhoff and co-workers[1,3,4].

Glass transition temperatures of copolymer films

The glass transition temperature (T_g°) of all the samples as obtained through d.s.c. is given in *Table 3* and *Figure 3*. Only one T_g° value was found for copolymer samples indicating that the samples were homogeneous copolymers and they were not blends of homopolymers of VA and BA. As seen from *Figure 3*, the T_g° decreased linearly with the increase of BA content.

Surface free energy components

Theory. The Young equation[26] describes the thermodynamic equilibrium of the three surface tensions, γ_{SV},

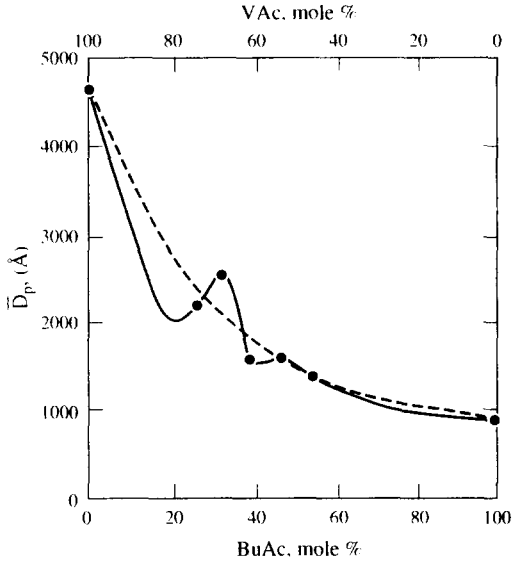

Figure 2 Change of the mean particle size with the BA content of VA–BA copolymers

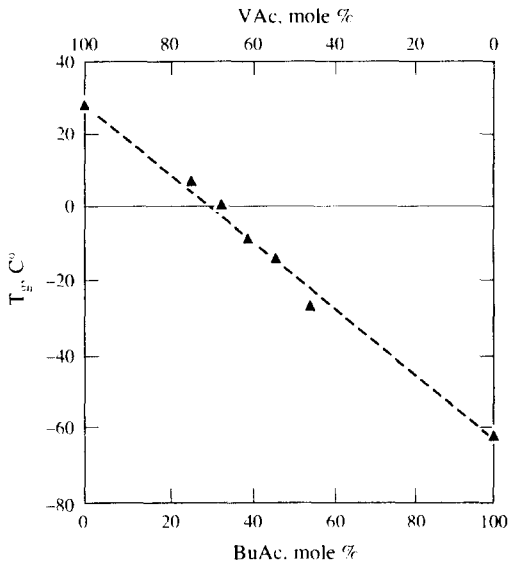

Figure 3 Change of the glass transition temperature with the BA content of VA–BA copolymers

γ_{SL}, γ_{LV}, existing at the phase boundaries of a drop of liquid at rest on a solid surface:

$$\gamma_{LV} \cos\theta = \gamma_{SV} - \gamma_{SL} \quad (2)$$

where γ_{LV}, γ_{SV}, γ_{SL} are respectively, the free energies of liquid, solid against their saturated vapour and of the interface between solid and liquid. Subscripts L, S and V refer to liquid, solid and vapour respectively. In this equation, the phases are supposed to be mutually in equilibrium and the spreading film pressure of the observed vapour of the liquid on the solid is neglected.

The work required to pull the liquid away from the surface leaving the equilibrium absorbed film (i.e. the total work of adhesion) is given by Dupre's equation[27]:

$$-\Delta G_A = W_A = \gamma_{SV} + \gamma_{LV} - \gamma_{SL} \quad (3)$$

Eliminating γ_{SL} from equations (2) and (3), the well-known

Young–Dupre equation is obtained:

$$W_A = \gamma_{LV}(1 + \cos\theta) \quad (4)$$

According to the Van Oss–Good theory[17–21], the surface and interfacial free energies (or tensions) consist of two components: an apolar or a Lifshitz–Van der Waals component (indicated by superscript LW) of electrodynamic origin, and a polar component caused by Lewis acid–base interactions (indicated by superscript AB). The two components are additive:

$$\gamma_{12}^{TOT} = \gamma_{12}^{LW} + \gamma_{12}^{AB} \quad (5)$$

They suggested that LW forces include not only the London dispersion forces (d) but also the Keesom orientation (p) and Debye induction (i) forces:

$$\gamma_{12}^{LW} = \gamma_{12}^{d} + \gamma_{12}^{p} + \gamma_{12}^{i} \quad (6)$$

For all exclusively LW interactions, i.e. interactions between two completely apolar compounds, the Good–Girifalco–Fowkes combining rule is applicable:

$$\gamma_{12}^{LW} = (\sqrt{\gamma_1^{LW}} - \sqrt{\gamma_2^{LW}})^2 \quad (7)$$

Between many liquid–solid interfaces in addition to LW interactions, polar interactions of the hydrogen-bonding type often occur. All electron acceptor–electron donor interactions or Lewis acid–base (AB) interactions are of this type. Unlike LW interactions, AB interactions are essentially asymmetrical and can only be satisfactorily treated by taking that asymmetry into account[17]. γ^{AB} component comprises two non-additive parameters. These are the electron-acceptor surface free energy component (designated as γ^+) and the electron-donor component (designated γ^-). These two parameters can be combined so that in the AB interaction between materials 1 and 2, the electron acceptor of 1 interacts with the electron donor of 2 and the electron donor of 1 interacts with the electron acceptor of 2. Thus, the free energy of AB interactions between 1 and 2 is expressed as:

$$-\Delta G_{12}^{AB} = W_{12}^{AB} = 2(\sqrt{\gamma_1^+\gamma_2^-} + \sqrt{\gamma_1^-\gamma_2^+}) \quad (8)$$

Now, since by definition

$$-\Delta G_A = (-\Delta G_{12}^{LW}) + (-\Delta G_{12}^{AB}) \quad (9)$$

and by combining equations (3) and (7) in LW form

$$-\Delta G_{12}^{LW} = W_{12}^{LW} = 2\sqrt{\gamma_1^{LW}\gamma_2^{LW}} \quad (10)$$

then, by combining equations (8), (9) and (10) one obtains

$$-\Delta G_A = W_A = 2(\sqrt{\gamma_1^{LW}\gamma_2^{LW}} + \sqrt{\gamma_1^+\gamma_2^-} + \sqrt{\gamma_1^-\gamma_2^+}) \quad (11)$$

Combining equations (4) and (11) and taking $\gamma_{LV} = \gamma_L$ as usual, the complete Young equation, comprising both the apolar and polar interactions, becomes:

$$\gamma_L(1 + \cos\theta) = 2(\sqrt{\gamma_S^{LW}\gamma_L^{LW}} + \sqrt{\gamma_S^+\gamma_L^-} + \sqrt{\gamma_S^-\gamma_L^+}) \quad (12)$$

Now, one can find the relation between γ^{AB} and its components γ^+ and γ^-. Dupre showed that the free energy of cohesion is:

$$-\Delta G_{11}^{coh} = 2\gamma_1 \quad (13)$$

For AB interactions equation (13) becomes

$$-\Delta G_{11}^{AB} = 2\gamma_1^{AB} \quad (14)$$

Now, if we express equation (8) in terms of 1 only,

$$-\Delta G_{11}^{AB} = 4\sqrt{\gamma_1^+\gamma_1^-} \quad (15)$$

From equations (14) and (15), it follows that,

$$\gamma_1^{AB} = 2\sqrt{\gamma_1^+\gamma_1^-} \quad (16)$$

Moreover, the total interfacial energy is given as[17]:

$$\gamma_{12}^{TOT} = (\sqrt{\gamma_1^{LW}} - \sqrt{\gamma_2^{LW}})^2 + 2(\sqrt{\gamma_1^+\gamma_1^-} + \sqrt{\gamma_2^+\gamma_2^-} - \sqrt{\gamma_1^+\gamma_2^-} - \sqrt{\gamma_1^-\gamma_2^+}) \quad (17)$$

Computation of the surface free energy components. γ_S^{LW} can be determined first by using apolar liquids. For an apolar liquid, $\gamma_L^+ = \gamma_L^- = 0$ and therefore $\gamma_L = \gamma_L^{LW}$. Then equation (12) can be written in the form:

$$\gamma_L(1 + \cos\theta) = 2\left(\sqrt{\gamma_S^{LW}\gamma_L}\right) \quad (18)$$

Consequently, the γ_S^{LW} value can be determined directly and the results of apolar liquid contact angles are averaged for a single value.

After this step, two polar liquids can be used to determine the remaining properties of the solid. For a polar liquid equation (12) can be written as

$$A = B\sqrt{\gamma_S^+} + C\sqrt{\gamma_S^-} \quad (19)$$

where

$$A = \gamma_L(1 + \cos\theta) - 2\sqrt{\gamma_S^{LW}\gamma_L^{LW}}$$
$$B = 2\sqrt{\gamma_L^-} \quad (20)$$
$$C = 2\sqrt{\gamma_L^+}$$

When two polar liquids are used, two equations of the form of equation (19) constitute a set of two simultaneous equations which can be solved for the two unknown properties of the solid γ_S^+ and γ_S^-. All γ_S^{LW}, γ_S^+, γ_S^- results are averaged for a single value.

Calculated results of surface free energy component of copolymer samples. Experimental contact angle results of probe liquids on copolymer samples are given in *Table 4*. The surface free energy component values of the used liquids and *B*, *C* values are given in *Table 5*[28]. The surface free energy components of copolymer samples calculated from equations (19) and (20) using the data given in *Tables 4* and *5* are given in *Table 6*. The Mathematica program (Version 2) was used to solve and average simultaneous equations.

Some negative square root results were obtained as the main defect of the Van Oss–Good theory, especially for

Table 4 Contact angles of probe liquids on copolymer samples (degrees)

Sample	BuAc (mol%)	Water	Glycerine	Ethylene glycol	Formamide	Decalin	Paraffin oil
P1	0	59	58	39	48	10	15
P2	26.8	61	60	43	57	14	17
P3	33.8	63	63	46	60	16	19
P4	40.0	70	65	49	62	18	21
P5	46.5	73	67	53	65	19	24
P6	55.4	75	67	54	68	21	26
P7	100.0	77	69	57	69	23	28

glycerine–formamide and ethylene glycol–formamide pairs, and were discarded. The other values seemed reasonable and were averaged. The change of γ_S^{LW} and γ_S^- with the increase of BA content of the copolymers is given in *Figure 4*. The change of γ_S^{AB} and γ_S^{TOT} with the increase of BA content is given in *Figure 5*.

In addition, the critical surface tension of copolymers was also determined using Zisman's method[29]. Zisman observed that $\cos\theta$ is usually a monotonic function of γ_L for a homologous series of liquids. The proposed function was:

$$\cos\theta = a - b\gamma_L = 1 - \beta(\gamma_L - \gamma_c) \qquad (21)$$

The lines in the plots of $\cos\theta$ *versus* γ_L extrapolates to zero θ ($\cos\theta = 1$) at a certain γ_L value which Zisman called the critical surface tension (γ_c) and proposed that γ_c was a quantity characteristic of a given solid. The old critical surface tension concept has provided a useful means of summarizing wetting behaviour; however, Zisman was careful to report that $\gamma_c \neq \gamma_{SV}$.

The γ_c values of copolymers were determined from the $\cos\theta$ *versus* γ_L plot taken from *Tables 4* and *5* in *Figure 6* (only P1, P3, P5 and P7 are shown in *Figure 6*). The critical surface tension values are reported in *Table 7*. The change of γ_c with increase of BA content of copolymers is given in *Figure 5*.

DISCUSSION

The surface functional groups on the latex particles could result from one or more of the following sources: (1) acetate groups of poly(VA) chains; (2) BA groups of poly(BA) chains; (3) hydroxyl groups from the hydrolysis of poly(VA) chains; (4) carboxylic acid groups form the hydrolysis of poly(BA) chains; (5) sulfite and sulfate groups from the initiator system; (6) nonyl phenol or ethoxyl groups from the emulsifier system.

The migration of surfactant molecules to the surface of polymer films cast from latexes were examined previously and it was found that nonyl phenol ethylene oxide emulsifiers do not exude to an appreciable extent due to the high compatibility between the polymer and the emulsifier[30,31]. On the other hand, it was shown using a.t.r. *FT*i.r. that sulfate groups were found in the region of the polymer surface[32]. Sulfate and carboxylic acid groups present on latex particles can be determined by the conductometric titration of the ion-cleaned latex samples using dilute sodium hydroxide solution[3,4]. It was found that for the semi-continuous latexes, the concentration of both sulfate and carboxyl groups decreased to a minimum and then increased with increasing BA content[1]. However, what portion of the sulfate, carboxyl and hydroxyl groups exude is still unknown for the films cast from latexes. In addition, in multicomponent polymers, it was reported that surface segregation occurs as the low surface tension component is preferentially

Table 5 Surface free energy component values of the liquids used (mJ m^{-2})[28]

	γ_L	γ_L^{LW}	γ_L^{AB}	γ_L^+	γ_L^-	B	C
Water	72.8	21.8	51.0	25.5	25.5	10.10	10.10
Glycerine	64.0	34.0	30.0	3.92	57.4	15.15	3.96
Ethylene glycol	48.0	29.0	19.0	1.92	47.0	13.71	2.77
Formamide	58.0	39.0	19.0	2.28	39.6	12.59	3.02
Decalin	29.9	29.9	0	0	0	0	0
Paraffin oil	28.9	28.9	0	0	0	0	0

Table 6 Surface free energy components of copolymer samples (mJ m^{-2})

Sample	BuAc (mol%)	γ_S^{LW}	γ_S^+	γ_S^-	γ_S^{AB}	γ_S^{TOT}
P1	0	28.7	0.90	38.53	11.8	40.5
P2	26.8	28.3	0.64	27.61	8.4	36.7
P3	33.8	28.5	0.48	24.13	6.8	35.3
P4	40.0	27.7	0.59	18.36	6.6	34.3
P5	46.5	27.4	0.41	19.53	5.7	33.1
P6	55.4	27.0	0.43	21.08	6.0	33.0
P7	100.0	26.6	0.47	11.97	4.7	31.3

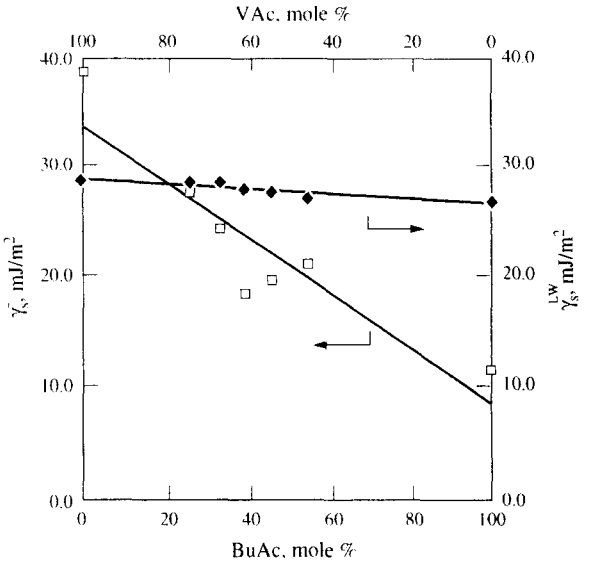

Figure 4 Change of the γ_S^{LW} and γ_S^- with the BA content of VA–BA copolymers

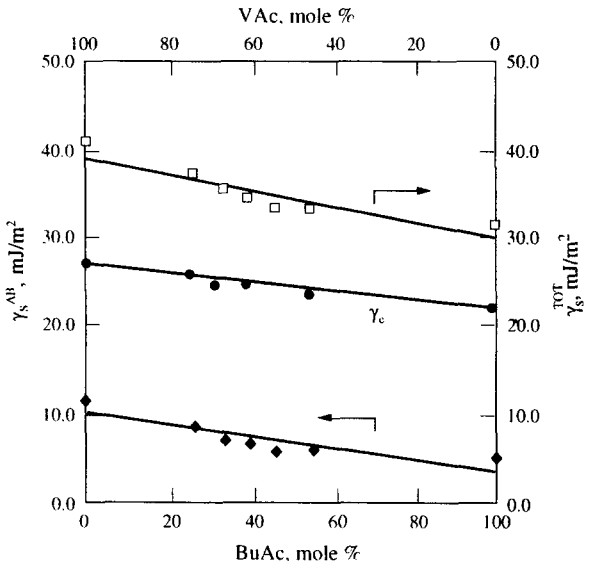

Figure 5 Change of γ_S^{AB}, γ_S^{TOT} and γ_c with the BA content of VA–BA copolymers

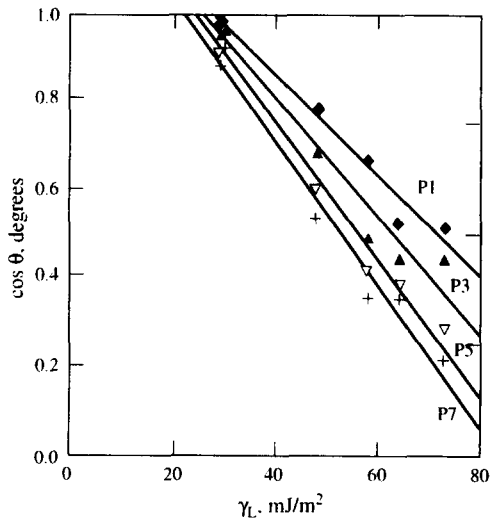

Figure 6 Determination of critical surface tension (γ_c) of copolymers from contact angle data

Table 7 Critical surface tension values of copolymer samples (mJ m^{-2})

Sample	γ_c
P1	27.2
P2	25.6
P3	24.6
P4	24.6
P5	23.7
P6	22.9
P7	21.9

enriched on the film surface[33,34]. The rearrangement of the polymer chain occurs according to the surface tension of the contacting material and the rate of rearrangement depends on the flexibility of the polymer chain. In our case the main focus of the surface energetics research is to evaluate the overall surface free energy of the copolymers with the change in BA content, since we kept the initiator, emulsifier, reaction times and the solids content of the final latex as constant parameters. Consequently, the films cast from the latexes exhibit the surface free energies arising from the groups from all the possible six sources mentioned above.

As was seen in *Figure 4*, a small decrease of γ_S^{LW} occurred with the increase of BA which was within ±3.8% deviation. However, the electron donor surface free energy coefficient (γ_S^-) decreased considerably with the BA increase in copolymer content so that 100% poly(BA) (P7) had only 31% of the initial value of 100% poly(VA) (P1). This decrease reflected the decrease of γ_S^{AB} and γ_S^{TOT} with the increase of BA content as seen in *Figure 5*. However, the γ_S^{AB} decrease is absorbed to some extent by the simultaneous decrease of γ_S^+ with the result that poly(BA) (P7) had only 40% of the γ_S^{AB} content of the poly(VA) (P1) as seen in *Figure 5*. It was also shown that the γ_S^{AB} contribution of copolymers in their total surface free energies (γ_S^{TOT}) was between 15 and 29% and the γ_S^{LW} contribution was between 71 and 85%. Consequently, the decrease of γ_S^{TOT} with the increase of BA content deviated within ±12.8% from the mean. For comparison, the change of the critical surface tension values (γ_c) taken from *Table 7* was also plotted in *Figure 5* and somewhat parallel decreases of γ_c and γ_S^{TOT} were seen with the increase of BA content. By comparison with *Figure 4* it is evident that γ_c shows a more similar trend to γ_S^{LW} indicating that the Zisman approach did not comprise acid–base interactions which are important in adhesive evaluation.

Adhesion of latex films to cellulose and cellulose acetate

The industrial production processes of poly(vinyl acetate) and vinyl acetate–butyl acrylate copolymer latexes are mainly semi-continuous and these latexes are commonly used as wood and paper adhesives and outdoor paints. Since most of the applied surfaces are cellulose based, a thermodynamic adhesion analysis is necessary between the cellulose surface and the latex film surface to understand practical adhesion which requires the knowledge of fundamental and thermodynamic adhesion as well as other adhesion factors[35]. (Other factors are the stresses present in the film and the substrate; the work consumed by plastic deformation and viscous dissipation, the mode of failure etc.) Mittal defined practical adhesion as the work required to remove or detach a film or coating from the substrate irrespective of the locus of failure which includes the energy required to deform both the film or coating and the substrate, as well as the energy dissipated as heat or stored in the film or coating[35]. On the other hand, the thermodynamic adhesion which is calculated from contact angle data gives information on the change in free energy when an interface is separated at the substrate–film interface. Although the adhesion failure may be cohesive rather than interfacial, or the failure process may involve localized deformation, knowledge of the thermodynamic work of adhesion would help in understanding practical adhesion since one may evaluate other adhesion factors more easily with the thermodynamic data at hand. In order to do so, the surface free energy components of cellulose and cellulose acetate are given in *Table 8*[36]. The total interfacial free energy and the work of adhesion between the copolymer films and the cellulose and cellulose acetate surfaces were calculated from equations (11) and (17) and are given

in Table 9. The change of the work of adhesion (W_A) with the change in BA content is given in *Figure 7*. As seen in this figure, W_A decreases with the increase of BA content indicating thermodynamically that the introduction of BA monomer weakens the work of adhesion between the copolymer films and cellulose and cellulose acetate surfaces. However, in practice, the introduction of BA has one more effect: it increases the wet-tack of the adhesive due to its lowering effect of T_g° or increasing effect of molecular motions at the application temperature.

CONCLUSION

The surface energetics of the films of poly(vinyl acetate–butyl acrylate) semi-continuous emulsion copolymers were studied. Non-ionic emulsifier, low temperature initiators and controlled comonomer initiator addition methods were used in the polymerizations resulting in copolymer compositions which deviated by only 0.7–5.2% from the feed monomer compositions. The change of the copolymer properties with the increase of BA content was as follows: viscosity-average molecular weights ($\bar{M}_V$) increased up to 40 mol% BA, then slowly decreased. The mean diameters of particles ($\bar{D}_p$) decreased showing that the more hydrophobic BA monomer favours the adsorption of emulsifier on the particle surface resulting in a higher number of small particles, whereas with increase in hydrophilic VA, coalescence occurs giving large particles. The glass transition temperature (T_g°) decreased linearly. The apolar Lifshitz–Van der Waals surface free energy component (γ_S^{LW}) of the latex film showed a small decrease within 3.8% deviation. However, the electron donor surface energy component (γ_S^-) decreased sharply. The acid–base interaction surface free energy component (γ_S^{AB}) and total surface free energy (γ_S^{TOT}) of the films as well as their critical surface tension (γ_c) all decreased slowly. The work of adhesion (W_A) of cellulose and cellulose acetate surfaces with the copolymer latex films and their interfacial free energies (γ_{12}) were also calculated and W_A was found to decrease with the increase of BA content.

Table 8 Surface free energy component values of cellulose and cellulose acetate[35] (mJ m^{-2})

	γ_S^{LW}	γ_S^+	γ_S^-	γ_S^{AB}	γ_S^{TOT}
Cellulose	39.1	2.0	39.7	17.6	56.7
Cellulose acetate	38.2	0.21	28.2	4.9	43.1

Table 9 Interfacial free energy and work of adhesion between cellulose, cellulose acetate and copolymer films (mJ m^{-2})

		P1	P2	P3	P4	P5	P6	P7
Cellulose	γ_{12}	0.89	2.15	2.84	3.58	3.95	3.71	5.34
	W_A	96.5	91.5	89.4	87.6	86.0	86.2	82.9
Cellulose acetate	γ_{12}	1.56	0.70	0.52	0.21	0.62	0.68	0.20
	W_A	82.0	79.1	77.9	77.1	75.6	75.4	74.2

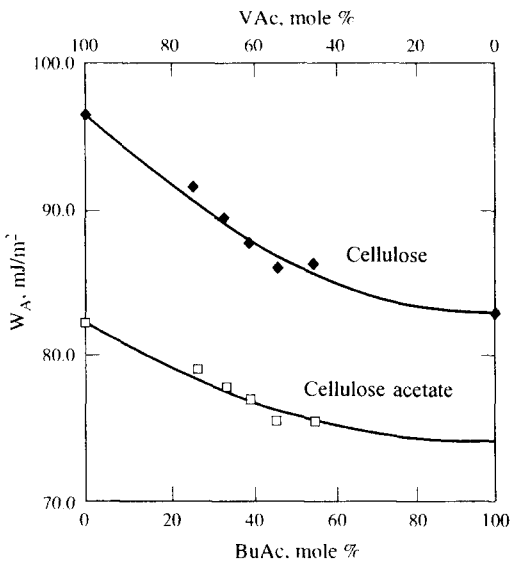

Figure 7 Change of W_A for cellulose and cellulose acetate with the BA content of VA–BA copolymers

REFERENCES

1 Vanderhoff, J. W. *J. Polym. Sci. Polym. Symp.* 1985, **72,** 161
2 Misra, S. C., Pichot, C., El-Aasser, M. S. and Vanderhoff, J. W. *J. Polym. Sci. Polym. Chem. Edn* 1983, **21,** 2383
3 El-Aasser, M. S., Makgawinta, T., Vanderhoff, J. W. and Pichot, C. *J. Polym. Sci. Polym. Chem. Edn* 1983, **21,** 2363
4 El-Aasser, M. S., Makgawinta, T., Misra, S. C., Vanderhoff, J. W., Pichot, C. and Llanro, M. F., in 'Emulsion Polymerization of Vinyl Acetate' (Eds M. S. El-Aasser and J. W. Vanderhoff), Applied Science, London, 1981, p. 215
5 Misra, S. C., Pichot, C., El-Aasser, M. S. and Vanderhoff, J. W. *Polym. Lett.* 1979, **17,** 567
6 Bataille, P. and Bourassa, H. *J. Polym. Sci. Polym. Chem. Edn* 1989, **27,** 357
7 Laurier, G. C., O'Driscoll, K. F. and Reilly, P. M. *J. Polym. Sci. Polym. Symp.* 1985, **72,** 17
8 Chujo, K., Harada, Y., Tokuhara, S. and Tanaka, K. *J. Polym. Sci.* 1969, **C27,** 321
9 Fowkes, F. M. *Ind. Eng. Chem.* 1964, **56,** 40
10 Girifalco, L. A. and Good, R. J. *J. Phys. Chem.* 1957, **61,** 904
11 Owens, D. K. and Wendt, R. C. *J. Appl. Polym. Sci.* 1969, **13,** 1741
12 Erbil, H. Y. *J. Appl. Polym. Sci.* 1987, **33**(4), 1397
13 Erbil, H. Y. *J. Appl. Polym. Sci.* 1988, **36,** 11
14 Erbil. H. Y. *Angew. Makromol. Chem.* 1987, **151,** 69
15 Erbil, H. Y. and Meriç, R. A. *Colloids Surf.* 1988, **33,** 85
16 Erbil, H. Y. and Meriç, R. A. *Angew. Makromol. Chem.* 1988, **163,** 101
17 Van Oss, C. J., Chaudhury, M. K. and Good, R. J. *J. Chem. Rev.* 1988, **88,** 927
18 Van Oss, C. J. and Good, R. J. *J. Macromol. Sci. Chem.* 1989, **A26,** 1183
19 Van Oss, C. J., Chaudhury, M. K. and Good, R. J. *Adv. Colloid Interface Sci.* 1987, **8,** 35
20 Van Oss, C. J. and Good, R. J. *J. Dispersion Sci. Technol.* 1991, **12,** 95
21 Van Oss, C. J. and Good, R. J. *Langmuir* 1992, **8,** 2877
22 Erbil, H. Y. *Langmuir* 1994, **10,** 286
23 Erbil, H. Y. *J. Colloid Interface Sci.* 1989, **129,** 384
24 Brandrup, J. and Immergut, E. H. (Eds) 'Polymer Handbook' 2nd edn, Wiley-Interscience, New York, 1975
25 Krackeler, J. J. and Naidus, H. *J. Polym. Sci.* 1969, **27C,** 207
26 Young, T. *Phil. Trans. Roy. Soc. (London)* 1805, **95,** 65
27 Dupre, A. 'Theorie Mecanique de la Chaleur', Gautier-Villars, Paris, 1869, p. 369
28 Van Oss, C. J., Giese, R. F., Li, Z., Murphy, K., Norris, J., Chaudhury, M. K. and Good, R. J. *J. Adhesion Sci. Technol.* 1992, **6,** 413
29 Zisman, W. A. *Adv. Chem. Ser.* 1964, **43,** 1
30 Zhao, C. L., Holly, Y., Pith, T. and Lambla, M. *Br. Polym. J.* 1989, **21,** 155

31 Evanson, K. W. and Urban, M. W. *J. Appl. Polym. Sci.* 1991, **42,** 2287
32 Eckersley, S. T., O'Daiskey, R. and Rudin, A. *J. Colloid Interface Sci.* 1992, **152,** 2, 455
33 Patel, N. M., Dwight, D. W., Hendrick, J. L., Webster, D. C. and McGrath, J. E. *Macromolecules* 1988, **21,** 2689
34 Kano, Y., Ishikura, K., Kawahara, S. and Akiyama, S. *Polym. J.* 1992, **24,** 135
35 Mittal, K. L. in 'Adhesion Measurement of Films and Coatings' (Ed. K. L. Mittal), VSP Press, Utrecht, 1995, p. 2
36 Toussaint, A. F. and Luner, P. in 'Contant Angle, Wettability and Adhesion' (Ed. K. L. Mittal), VSP Press, Utrecht, 1993, p. 383